

Electric-field-induced melting of the randomly pinned charge-ordered states of rare-earth manganates and associated effects

C. N. R. Rao,* A. R. Raju, V. Ponnambalam, and Sachin Parashar

Chemistry and Physics of Materials Unit, Jawaharlal Nehru Centre for Advanced Scientific Research, Jakkur P.O., Bangalore 560 064, India

N. Kumar

Raman Research Institute, Bangalore 560 080, India

(Received 30 November 1998; revised manuscript received 31 August 1999)

Films of charge-ordered $\text{Nd}_{0.5}\text{Ca}_{0.5}\text{MnO}_3$, $\text{Gd}_{0.5}\text{Ca}_{0.5}\text{MnO}_3$, $\text{Y}_{0.5}\text{Ca}_{0.5}\text{MnO}_3$, and $\text{Nd}_{0.5}\text{Sr}_{0.5}\text{MnO}_3$ show insulator-metal transitions on the passage of small electrical currents. That such an electric-field-induced transition occurs even in $\text{Y}_{0.5}\text{Ca}_{0.5}\text{MnO}_3$ where the charge-ordered state is not affected by magnetic fields is noteworthy. The transition is attributed to the depinning of the randomly pinned charge solid. These materials also exhibit an interesting memory effect probably due to the randomness of the strength as well as the position of the pinning centers.

I. INTRODUCTION

Charge ordering in some of the compositions of rare-earth manganates of the formula $L_{1-x}A_x\text{MnO}_3$ (L =rare earth, A =alkaline earth) has been well-documented.^{1,2} Charge ordering in these materials is interesting since it competes with double exchange, giving rise to several interesting properties. The charge-ordered state is insulating unlike the double-exchange regime of the manganates. Two types of charge ordering can be distinguished in the manganates.^{2,3} In $\text{Nd}_{0.5}\text{Sr}_{0.5}\text{MnO}_3$ with a relatively large average radius of the A -site cations, $\langle r_A \rangle$, a ferromagnetic metallic (FMM) state ($T_c=250$ K) transforms to a charge-ordered (CO) state on cooling to ~ 150 K.⁴ Manganates with a small $\langle r_A \rangle$ (≤ 1.17 Å) do not exhibit the FMM state at any temperature and instead occur in the CO state even at relatively high temperatures. The CO state in a manganate with a relatively large A -site ion radius ($\langle r_A \rangle \geq 1.17$ Å) can be transformed to the FMM state by the application of magnetic fields. On the other hand, even large magnetic fields have negligible effect on the CO state of $\text{Y}_{0.5}\text{Ca}_{0.5}\text{MnO}_3$ with a $\langle r_A \rangle$ of 1.13 Å.⁵ The CO state in single crystals of $\text{Pr}_{1-x}\text{Ca}_x\text{MnO}_3$ has been transformed to the FMM state by applying electric fields and/or laser irradiation.^{6,7} The effect of electric fields on the CO state of the manganates clearly requires a thorough investigation, not only because of interesting features of the phenomenon but also due to possible technological implications.

There has been little effort to prepare and characterize thin films of the charge-ordered manganates, unlike the thin films of the manganates showing CMR.⁸⁻¹¹ We have prepared thin films of charge-ordered manganates of the general composition $L_{0.5}A_{0.5}\text{MnO}_3$ on single-crystal substrates by the nebulized spray pyrolysis of organometallic precursors. More significantly, we have investigated the electric current-induced transition of the insulating CO states to metal-like states in these films. For the purpose of this study, we have chosen three manganates at half doping of the composition

$L_{0.5}\text{Ca}_{0.5}\text{MnO}_3$ with $L=\text{Nd}$, Gd , and Y with $\langle r_A \rangle$ values of 1.17, 1.14, and 1.13 Å, respectively, as well as $\text{Nd}_{0.5}\text{Sr}_{0.5}\text{MnO}_3$ with a $\langle r_A \rangle$ of 1.24 Å. It is noteworthy that the insulating CO state in all these manganates, including $\text{Y}_{0.5}\text{Ca}_{0.5}\text{MnO}_3$, is melted by passing small currents. Furthermore, the films show nonohmic behavior and interesting memory effects. We propose that the electric-field-induced insulator-metal transitions and associated effects are brought about by the depinning of the randomly pinned charge solids.

II. EXPERIMENTAL

Thin films of the manganates were deposited on Si(100) as well as on lanthanum aluminate, LAO(100), single crystal substrates by employing nebulized spray pyrolysis.¹² This technique involves the pyrolysis of a nebulized spray of organic derivatives of the relevant metals. Since the nebulized spray is deposited on a solid substrate at relatively low temperatures, and with sufficient control of the rate of deposition, the oxide films obtained possess good stoichiometry. Employing acetylacetonates of Nd, Gd, Y, Ca, and Mn, and dipivaloylmethanato strontium as the organometallic precursors, films of ~ 1000 nm thickness were deposited at 650 K by using air as the carrier gas (1.5 liters/min). The films so obtained were heated at 1000 K in oxygen. The films were characterized by employing x-ray diffraction and scanning electron microscopy. The compositions of the films as determined by EDAX were close to the stated compositions. The films deposited on Si(100) showed a polycrystalline nature while those deposited on LAO were oriented along the (100) direction. The orthorhombic lattice parameters of the materials agree with the literature values. Temperature-dependent resistivity measurements were carried out by employing a close cycle refrigerator and sputtered gold electrodes.

III. RESULTS

In Figs. 1(a) and 1(b), we show the temperature variation of the resistance of $\text{Nd}_{0.5}\text{Ca}_{0.5}\text{MnO}_3$ (NCM) films deposited

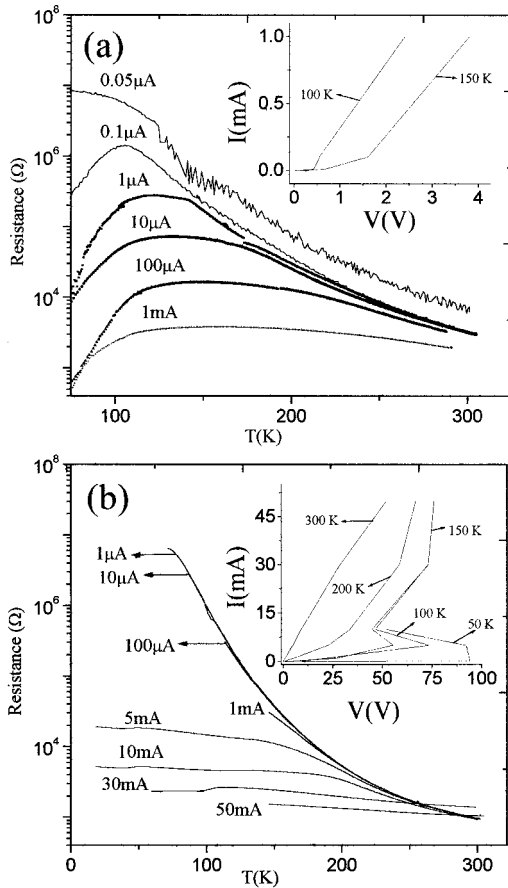


FIG. 1. Temperature variation of the resistance of $\text{Nd}_{0.5}\text{Ca}_{0.5}\text{MnO}_3$ (NCM) films deposited on (a) Si(100) and (b) LAO(100) for different values of current. The insets show I - V characteristics at different temperatures.

on Si(100) and LAO(100), respectively, for different values of the dc current passed. When the current is small ($0.05 \mu\text{A}$), the film on Si(100) shows insulating behavior. Upon increasing the current, we observe the occurrence of an insulator-metal (I-M) transition (Fig. 1(a)). It is noteworthy that even a current of $0.1 \mu\text{A}$ causes the I-M transition. (The values of the current density are 1.25 A cm^{-2} and $1.25 \times 10^4 \text{ A cm}^{-2}$ for currents of $1 \mu\text{A}$ and 10 mA , respectively.) The effects observed are not due to local Joule heating, which becomes appreciable only at high currents ($\geq 50 \text{ mA}$). In fact, the irrelevance of the Joule heating can be clearly seen in the low-temperature metallic [temperature coefficient of resistance (TCR) > 0] regime accessible in Fig. 1(a). Here the resistance for a given current increases with increasing temperature, while for a given temperature the resistance decreases with increasing current. Just the opposite would be true for a Joule heating. It is reasonable, therefore, to assume that the Joule heating is quite irrelevant to our transport results, qualitatively at least. The temperature of the I-M transition shifts from 100 to 150 K with increase in current. The I - V curves show nonohmic behavior as shown in the inset of Fig. 1(a). Measurements on the oriented NCM film deposited on LAO(100) also shows a marked decrease in resistance with increasing current (Fig. 1(b)). We do not clearly see a metal-like decrease in resistance at low temperatures, and the behavior is comparable to that of laser-irradiated $\text{Pr}_{1-x}\text{Ca}_x\text{MnO}_3$ crystals reported by

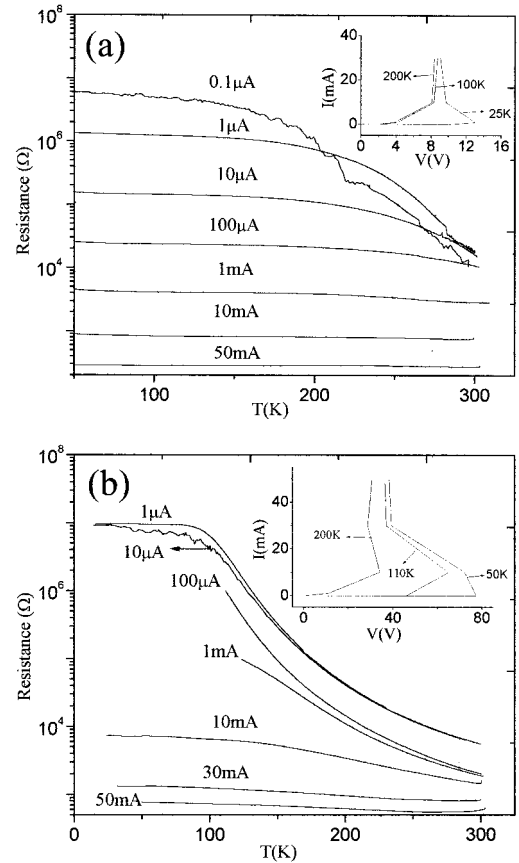


FIG. 2. Temperature variation of the resistance of $\text{Gd}_{0.5}\text{Ca}_{0.5}\text{MnO}_3$ (GCM) films deposited on (a) Si(100) and (b) LAO(100) for different values of current. The insets show I - V characteristics at different temperatures.

Ogawa *et al.*⁷ The oriented NCM films also show nonohmic behavior [see inset of Fig. 1(b)]. On the LAO substrate, a higher current is required to reduce the resistance of the NCM film to the same extent as on the Si substrate.

In Figs. 2(a) and 2(b), we show the effect of increasing the electric current on the resistance of $\text{Gd}_{0.5}\text{Ca}_{0.5}\text{MnO}_3$ (GCM) films deposited on Si(100) and LAO(100) substrates, respectively. The behavior is comparable to that of NCM films, particularly on the LAO substrate. On the Si(100) substrate, the GCM films show essentially flat resistance curves with almost no change with temperature, reminiscent of degenerate materials. This is specially noticeable when the current is $\geq 100 \mu\text{A}$. On the LAO(100) substrate, such near constancy of resistance is seen when the current is greater than 10 mA . Nonohmic behavior is found in the GCM films as well, as can be seen from the insets in Figs. 2(a) and 2(b).

A particularly remarkable feature of the NCM and GCM films deposited on LAO(100) substrates is the occurrence of a hysteretic I-M transition driven by transport current. We show typical data on these films in Fig. 3. The resistance-temperature plots (at constant transport current) are as described earlier when the sample is cooled from room temperature. After attaining the lowest temperature of measurement ($\sim 20 \text{ K}$) the current is switched off, and switched on again to carry out measurements as the films are heated. Note that at the current switching, the large resistance increase overloads the available current source used.

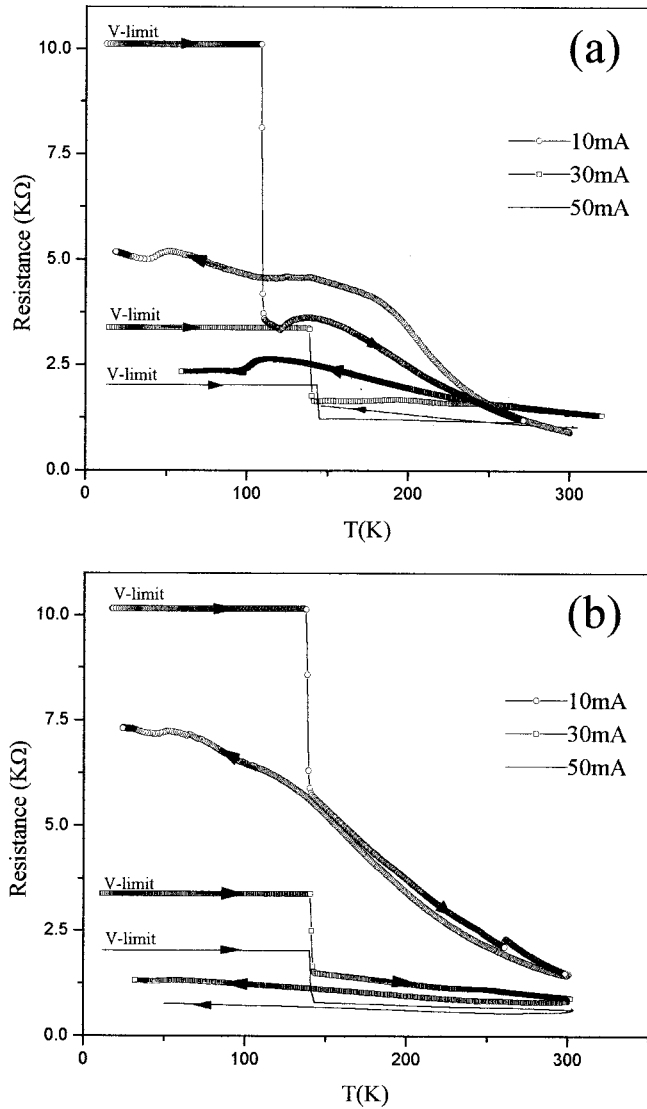


FIG. 3. Resistance versus temperature plots of (a) $\text{Nd}_{0.5}\text{Ca}_{0.5}\text{MnO}_3$ and (b) $\text{Gd}_{0.5}\text{Ca}_{0.5}\text{MnO}_3$ films deposited on LAO(100) for three different current values, recorded over cooling and heating cycles. The current was switched off after cooling curve was completed and turned on again to record the heating curve.

Our current source overload was 105 V, thus causing overload when the resistance is 105 M Ω for a current of 10 mA. (We do not have a source of higher voltage.) The heating curves first show an abrupt increase in resistance followed by an equally abrupt drop around a temperature at which the charge solid apparently melts. The jump in resistance to the original value on the cooling curve in the charge liquid state is indeed remarkable. Such a memory of the current-specific resistance value registered in the charge liquid state is an interesting property.

In Fig. 4(a), we show the resistance vs temperature curves of a $\text{Y}_{0.5}\text{Ca}_{0.5}\text{MnO}_3$ (YCM) film on LAO(100) for different values of the current. We observe a substantial decrease in the resistance with increase in the current and the I - V behavior is nonohmic [see inset of Fig. 4(a)]. The occurrence of a current-induced I-M-type transition in the YCM film is noteworthy as the CO state in this material is very robust, being

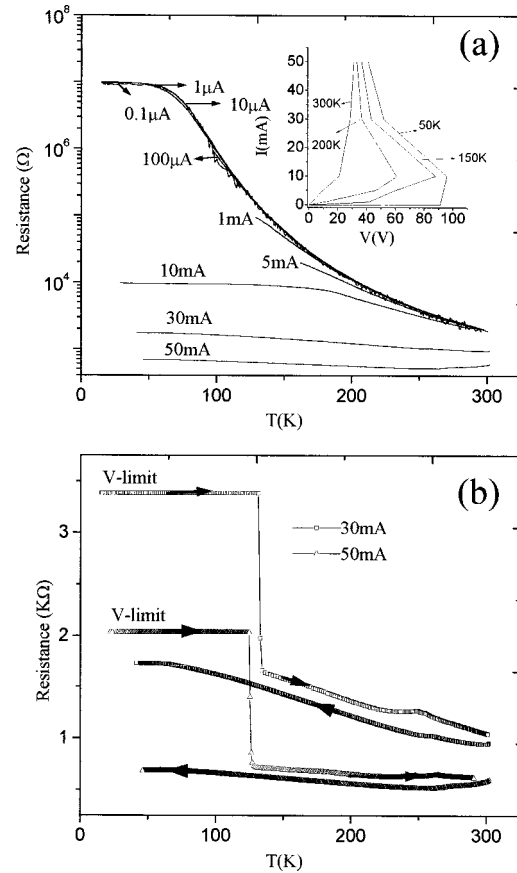


FIG. 4. (a) Temperature variation of the resistance of a $\text{Y}_{0.5}\text{Ca}_{0.5}\text{MnO}_3$ (YCM) film deposited on LAO(100) for different values of current. The inset shows I - V characteristics at different temperatures. (b) Cooling and heating curves obtained as described in the caption of Fig. 3.

unaffected by magnetic fields or substitution of Mn^{3+} by Cr^{3+} and such ions.^{3,5,13} The value of resistance at a given current varies as $\text{YCM} > \text{GCM} > \text{NCM}$, in the same order as the $\langle r_A \rangle$. The memory effect discussed earlier is also found in the YCM film, as shown in Fig. 4(b).

In Fig. 5, we show the temperature variation of resistance of a $\text{Nd}_{0.5}\text{Sr}_{0.5}\text{MnO}_3$ (NSM) film deposited on Si(100). The NSM films show metallic resistivity from ~ 300 K down to ~ 140 K and resistance increases below 140 K due to charge ordering. The increase in resistance in the CO state is not as sharp in the film as in a single crystal.⁴ We, however, observe the high-temperature metallic behavior for all current values and the resistance decreases substantially in the charge-ordering regime, with increasing current. At 50 mA, the material remains metallic from 300 to 20 K, although there is a slight heating of the sample at this current value. The resistance values in NSM are considerably lower than in NCM and other films at similar currents. The NSM film also shows nonohmic behavior (see inset of Fig. 5). Mori¹⁴ has recently observed effects in NSM crystals somewhat comparable to the memory effects [Figs. 3 and 4(b)] found by us.

IV. DISCUSSION

We discuss now the electric-field-induced insulator-metal transition and the nonohmic transport in the charge-ordered

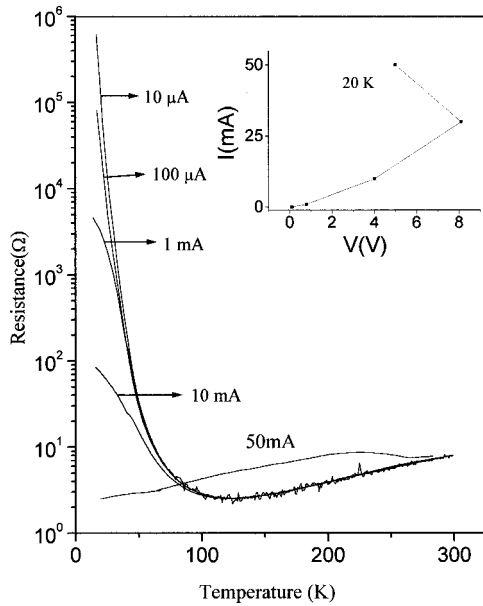


FIG. 5. Temperature variation of the resistance of a $\text{Nd}_{0.5}\text{Sr}_{0.5}\text{MnO}_3$ (NSM) film deposited on Si(100) for different values of current. The inset shows I - V characteristic at a low temperature.

rare-earth manganates. These materials are to be viewed as charge solids pinned randomly to the underlying lattice, and can be depinned by an externally applied electric field, and, of course, melted thermally. The random pinning is expected on general grounds, e.g., the L/A substitutional disorder in $L_{0.5}A_{0.5}\text{MnO}_3$ that acts as a quenched randomness, other lattice defects or possible inhomogeneities, including the occurrence of domains or clusters of CO and metallic phases. Charge ordering in the cubic manganates is, however, not a charge-density wave (CDW) arising from a nesting of the Fermi surface and the associated Peierls instability, as presumably is the case for the effectively low-dimensional layers system,¹⁵ Sr_2IrO_4 . Charge ordering in the manganates is driven by Coulomb interaction among the charge carriers, and is stabilized by the background lattice potential, with which it is ideally commensurate for the 1/1 ordered $\text{Mn}^{3+}/\text{Mn}^{4+}$ case. The charge carriers themselves are expected to be polarons—specifically, the lattice polarons associated with the Jahn-Teller ions Mn^{3+} for the manganates with a small average A -cationic radius as, e.g., in NCM, YCM, or GCM. Charge transport in these manganates, again unlike a CDW with its sliding or unpinned condensate, is expected to proceed through the correlated motion of the polarons, depinned by the applied electric field. This picture is qualitatively consistent with the observed facts, namely, the observed threshold of electric field, or applied current, for electrical conduction, nonohmic transport, metal-insulator transition, negative differential resistance, and certain hysteretic and memory effects associated with the melting transition from a charge solid to a charge liquid as discussed below.

At the lowest temperature (77 K) and current ($I \leq 0.05 \mu\text{A}$) employed, the NCM film [Fig. 1(a)] is highly insulating ($\text{TCR} < 0$) with $R \sim 10^7 \Omega$. The resistance then falls by an order of magnitude for a small increase of the current to $\sim 0.1 \mu\text{A}$, but finally levels off to a gradual de-

crease around 1 mA. The corresponding variation in the applied voltage, and, therefore, of the electric field, is small, from ~ 0.5 to ~ 0.6 V. This nonlinear threshold conduction, qualitatively of the Zener type $R \propto \exp(E_0/E)$, is characteristic of a pinned charge solid (insulator), and its field-induced depinning gives a conductor. The field-induced depinning also accounts for the nonohmic decrease of resistance with increasing applied current at a given temperature as observed in these manganates. Let us next consider the temperature dependence of resistance at a given current. At low enough temperatures, the depinning energy far exceeds the thermal energy ($k_B T$) and the conduction is dominated by a coherent tunneling step. A positive TCR is to be expected because of the decohering thermal effects, as indeed observed [Fig. 1(a)]. At higher temperatures, the transport crosses over from this quantum coherent tunneling through pinning barrier to an incoherent thermal escape over the barrier giving a change in sign of the TCR (< 0) as expected of a thermally activated process. This is again exactly what is observed [Fig. 1(a)]. Indeed, such a crossover from a low-temperature coherent conduction with a positive TCR to a higher temperature incoherent conduction with a negative TCR is well known for independent small polarons. In the present case, the single polaron is replaced by the polarons entrained in a correlation volume due to interaction. With increasing temperature, the coherence volume must decrease thereby lowering the depinning energy. It is very apt to point out here that the field-induced depinning of the randomly pinned charge solid has a close analogue in the well-known phenomenon of shear induced melting, which is not the result of heating.

The picture discussed above with reference to Fig. 1(a) for NCM/Si also covers the NCM/LAO, GCM/Si or LAO, and YCM/LAO films depicted in Figs. 1(b), 2, and 4(a), respectively. In these cases, the metallic-type regime with $\text{TCR} > 0$ (found in NCM/Si at low temperatures) is absent. This suggests that the correlation volume, or the pinning barrier, is sufficiently small for the thermally activated depinning to dominate over tunneling even at low temperatures, thus making the regime with $\text{TCR} > 0$ parametrically inaccessible. In the case of NSM (Fig. 5), charge ordering and its pinning involve antiferromagnetic (AFM) ordering, and hence the depinning occurs at relatively lower temperatures. The idea of pinning/depinning, and of the associated coherence volume entraining a number of charge carriers, is general and has a much wider applicability. Thus, it is applicable to the classic Wigner crystal pinned by random substrate imperfections, to which the CO state considered here approximates best—but with the proviso that the electrons have to be replaced by JT polarons whose higher effective mass favors charge solid formation in the parameter regime of interest.

The negative differential resistance in the case of the magnetic CO manganates (as in NSM) can be understood in terms of local ferromagnetic (FM) ordering forced by a sufficiently large transport current impressed as an external constraint. This is the spin-valve effect acting in the reverse, assuming that the Hund's coupling is far larger than the antiferromagnetic coupling. The transport-induced local FM order leads to a lower resistance because of the spin-valve effect, and hence the negative differential conductance. Such

a transport driven (magnetic) structural change is a particular case of the general nonequilibrium phenomenon of ordering caused by transport. Similar transport driven instability is expected in the other systems showing negative differential conductance.

Finally, we turn to the remarkable hysteretic I-M transitions driven by the transport current in the CO systems shown in Figs. 3 and 4(b) and described in Sec. III. The R - T plot at constant transport current along the heating curve shows an abrupt drop at the transition temperature (~ 150 K) at which clearly the charge solid melts to a charge liquid. On the cooling curve, the charge liquid shows appreciable undercooling (stays liquid below ~ 150 K) which is not surprising for a melting transition. What is surprising, however, is that on the heating curve (following the switching of the applied current at the lowest temperature) the resistance jumps back at melting to its original current-specific value on the cooling curve in the charge liquid melt. This memory of the current specific-resistance value registered in the charged

liquid state, and addressed uniquely by that specific value of the transport current, can be understood in terms of the quenched randomness of the strength as well as the position of the pinning referred to earlier.¹⁶ Accordingly, at a given transport current, the charge solid is depinned only at a subset of pinning centers. We suggest that effectively only this depinned fraction melts cooperatively at the melting point, and then contributes to the conductance in the charge liquid state. This subset increases with the increasing applied current, giving therefore, lower resistance for higher currents in the charge liquid state, as is clearly seen in Figs. 2 and 4(b). (Here again, the Joule heating is irrelevant as is evident from the fact that the observed melting temperature is unaffected by the applied current magnitude.) Thus, the charge liquid just above the melting temperature also conducts nonohmically. It is the transport-current specificity of the charge liquid resistance that sets it apart from the hysteresis usually associated with the first-order melting transition.

*Electronic address: cnrrao@jncasr.ac.in

- ¹Y. Tokura, in *Colossal Magnetoresistance, Charge-Ordering and Related Properties of Manganese Oxides*, edited by C. N. R. Rao and B. Raveau (World Scientific, Singapore, 1998); Y. Tokura, *Curr. Opin. Solid State Mater. Sci.* **4**, 175 (1998); Y. Tokura, Y. Tomioka, H. Kuwahara, A. Asamitsu, Y. Moritomo, and M. Kasai, *J. Appl. Phys.* **79**, 5288 (1996); A. P. Ramirez, *J. Phys.: Condens. Matter* **9**, 8171 (1997).
- ²C. N. R. Rao, A. Arulraj, P. N. Santosh, and A. K. Cheetham, *Chem. Mater.* **10**, 2714 (1998).
- ³A. Arulraj, P. N. Santhosh, A. Guha, A. K. Raychaudhuri, N. Kumar, and C. N. R. Rao, *J. Phys.: Condens. Matter* **10**, 8497 (1998).
- ⁴H. Kuwahara, Y. Tomioka, A. Asamitsu, Y. Moritomo, and Y. Tokura, *Science* **270**, 961 (1995).
- ⁵A. Arulraj, R. Gundakaram, A. Biswas, N. Gayathri, A. K. Raychaudhuri, and C. N. R. Rao, *J. Phys.: Condens. Matter* **10**, 4447 (1998).
- ⁶A. Asamitsu, Y. Tomioka, H. Kuwahara, and Y. Tokura, *Nature (London)* **388**, 50 (1997).
- ⁷K. Ogawa, W. Wei, K. Miyano, Y. Tomioka, and Y. Tokura,

- Phys. Rev. B* **57**, R15 033 (1998); M. Fiebig, K. Miyano, Y. Tomiyoka, and Y. Tokura, *Science* **280**, 1925 (1998).
- ⁸J. Q. Wang, R. C. Barker, G. J. Cui, T. Tamagawa, and B. L. Halpern, *Appl. Phys. Lett.* **71**, 3418 (1997).
- ⁹A. R. Raju, H. N. Aiyer, B. V. Nagaraju, R. Mahendiren, A. K. Raychaudhuri, and C. N. R. Rao, *J. Phys. D: Appl. Phys.* **30**, L71 (1997).
- ¹⁰J. G. Snyder, R. Hiskes, S. DiCarolis, M. R. Beasley, and T. H. Geballe, *Phys. Rev. B* **53**, 14 434 (1996).
- ¹¹G. C. Xiong, Q. Li, H. L. Ju, R. L. Green, and T. Venkatesan, *Appl. Phys. Lett.* **66**, 1689 (1995).
- ¹²H. N. Aiyer, A. R. Raju, G. N. Subbanna, and C. N. R. Rao, *Chem. Mater.* **9**, 755 (1997); A. R. Raju and C. N. R. Rao, *Appl. Phys. Lett.* **66**, 896 (1995).
- ¹³P. V. Vanitha, R. S. Singh, S. Natarajan, and C. N. R. Rao, *J. Solid State Chem.* **137**, 365 (1998).
- ¹⁴T. Mori, *Phys. Rev. B* **58**, 12 543 (1998).
- ¹⁵G. Grüner, *Rev. Mod. Phys.* **60**, 1129 (1988).
- ¹⁶G. Cao, J. Bolivar, S. McCall, J. E. Crow, and R. P. Guertin, *Phys. Rev. B* **57**, R11 039 (1998).